Acta Crystallographica Section F
Structural Biology and Crystallization Communications
ISSN 1744-3091

Crystallization and preliminary X-ray crystallographic analysis of MinE, the cell-division topological specificity factor from *Helicobacter pylori*

Gil Bu Kang, Hye-Eun Song, Mun-Kyoung Kim, Hyung-Seop Youn, Jun Yop An, Jung-Gyu Lee, Kyung Ryung Park and Soo Hyun Eom*

Department of Life Science, Gwangju Institute of Science and Technology, Gwangju 500-712, Republic of Korea

Correspondence e-mail: eom@gist.ac.kr

Received 20 January 2010
Accepted 16 March 2010

Cell division in Gram-negative bacteria is driven by the formation of an FtsZ ring at the division site. MinE regulates the proper placement of the FtsZ ring at mid-cell by blocking the inhibitory action of the MinCD complex. Diffraction data were collected at 2.8 Å resolution from a native crystal of full-length *Helicobacter pylori* MinE. The crystal belonged to space group $P6_4$. Assuming the presence of two molecules in the asymmetric unit, the calculated Matthews coefficient was 2.58 Å^3 Da^{-1}, which corresponds to a solvent content of 52.3%. For MAD phasing, a four-wavelength data set was collected at 3.0 Å resolution.

1. Introduction

In most organisms, cell division proceeds with the placement of a septum through the mid-cell region, permitting an equal distribution of the cellular compartments into the two daughter cells (Rothfield *et al.*, 2005). This process is driven by the formation of an FtsZ ring at the division site. In Gram-negative bacteria, including *Escherichia coli*, the proper placement of the FtsZ ring is mediated by nucleoid occlusion and the dynamic oscillating Min proteins (MinC, MinD and MinE; RayChaudhuri *et al.*, 2000; Moller-Jensen & Lowe, 2005; Gitai, 2007).

The three Min proteins act in concert to prevent septum formation at sites other than the mid-cell region. MinC and MinD form a MinCD complex, which acts as a nonspecific division inhibitor that blocks septation at all potential division sites. The complex oscillates from one pole of the cell to the other, thereby causing a periodic block to cell division (Raskin & de Boer, 1999). MinE protects the mid-cell division site from inhibition by MinCD by localizing to a ring-like structure (the E-ring) in the mid-cell region (Raskin & de Boer, 1997). Inhibition of the activity of the MinCD complex in the vicinity of this ring reflects the ability of MinE to induce dissociation of the complex (Huang *et al.*, 1996).

MinE has two structurally and functionally distinct domains: the anti-MinCD domain and the topological specificity domain (TSD; Pichoff *et al.*, 1995; Zhao *et al.*, 1995). The TSD (residues 32–88) of *E. coli* MinE is required for E-ring formation, while the anti-MinCD domain (residues 1–31) interacts with MinD to dissociate the MinCD complex, thereby blocking the inhibitory effect of MinC on cell division. Despite the importance of the role played by MinE in bacterial cell division, little structural information is available about this protein. Only the solution structure of a truncated form of *E. coli* MinE (residues 32–88) has been determined (King *et al.*, 2000). As a result of this lack of structural information, the functions of MinE, including the MinE–MinD interaction that inhibits the MinCD complex and MinE ring formation, are not well understood.

A better understanding of the biological functions of MinE will require determination of the high-resolution structure of full-length MinE. As a first step towards this goal, we report the overexpression, purification and crystallization of full-length *Helicobacter pylori* MinE and its preliminary X-ray characterization.

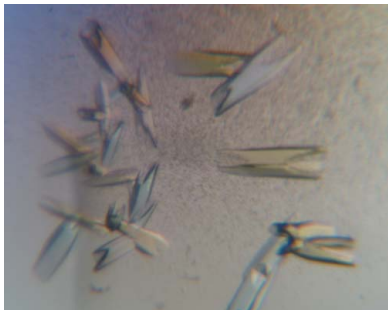

Table 1
Data-collection and processing statistics.

Values in parentheses are for the highest resolution shell.

		SeMet derivative			
	Native	Inflection	Peak	Remote 1	Remote 2
No. of crystals	1	1			
Beamline	PAL 4A	PF BL5			
Wavelength (Å)	1.0000	0.9796	0.9791	0.9833	0.9644
Detector	ADSC Quantum 210 CCD	ADSC Quantum 315 CCD			
Crystal-to-detector distance (mm)	250	400			
Rotation range per image (°)	1	1			
Total rotation range (°)	300	240			
Exposure time per image (s)	10	15			
Resolution range (Å)	50–2.8 (2.85–2.80)	50–3.0 (3.05–3.00)			
Space group	$P6_4$	$P6_5$			
Unit-cell parameters (Å)	$a = b = 70.8$, $c = 65.5$	$a = b = 38.1$, $c = 153.5$			
Mosaicity (°)	0.66	0.81	0.82	0.79	0.82
Total No. of measured intensities	43987	38789	38521	38253	38310
Unique reflections	4582	2751	2732	2713	2717
Multiplicity	9.6 (9.7)	14.1 (12.5)	14.1 (13.0)	14.1 (12.6)	14.1 (13.3)
$\langle I/\sigma(I)\rangle$	17.4 (5.6)	15.6 (3.9)	15.4 (4.4)	15.9 (3.9)	14.8 (3.5)
Completeness (%)	99.7 (100)	98.2 (89.4)	97.9 (84.1)	98.3 (92.6)	97.5 (82.8)
$R_{\rm merge}$† (%)	7.2 (41.5)	6.3 (56.1)	6.6 (52.8)	5.9 (50.5)	6.7 (56.0)
Overall B factor from Wilson plot (Å^2)	84.1	99.1	96.8	99.4	96.6

† $R_{\rm merge} = \sum_{hkl}\sum_i |I_i(hkl) - \langle I(hkl)\rangle| / \sum_{hkl}\sum_i I_i(hkl)$, where $I_i(hkl)$ is the intensity of the ith observation of reflection hkl and $\langle I(hkl)\rangle$ is the average intensity of reflection hkl.

2. Materials and methods

2.1. Expression and purification

DNA encoding full-length *H. pylori* MinE (residues 1–77; Gene ID 899209) was amplified by PCR and subcloned into the *Nde*I and *Xho*I sites of the expression vector pET-28b (Novagen), which resulted in the addition of an N-terminal His tag to the expressed protein. After transformation into *E. coli* strain BL21 (DE3), recombinant *H. pylori* MinE was induced by treating the cells with 1 m*M* isopropyl *β*-D-1-thiogalactopyranoside (IPTG) for 16 h at 293 K. The cells were harvested and resuspended in lysis buffer containing 50 m*M* sodium phosphate pH 7.5, 300 m*M* NaCl; the suspended cells were then lysed by sonication and centrifuged at 14 000*g* for 1 h. The supernatant was collected and loaded onto a column packed with Ni–NTA resin (Peptron) pre-equilibrated with lysis buffer. After washing with wash buffer (50 m*M* sodium phosphate pH 7.5, 300 m*M* NaCl, 10 m*M* imidazole), the bound protein was eluted with elution buffer (50 m*M* sodium phosphate pH 7.5, 300 m*M* NaCl, 300 m*M* imidazole). The N-terminal His tag was then removed using thrombin. The digested *H. pylori* MinE protein, which included an extra three residues (GSH) at the N-terminus as a result of the gene cloning, was further purified by size-exclusion chromatography on a Superdex 75 column (Pharmacia) equilibrated with 20 m*M* Tris–HCl pH 6.0, 150 m*M* NaCl. The fractions containing the recombinant protein were pooled and concentrated to 20 mg ml^{-1} using a Centriprep-3 (Amicon).

Selenomethionine-labelled protein was overexpressed in *E. coli* strain B834 (DE3) cultured in M9 medium supplemented with selenomethionine (SeMet) and was purified using the same protocol as was used for the native *H. pylori* MinE.

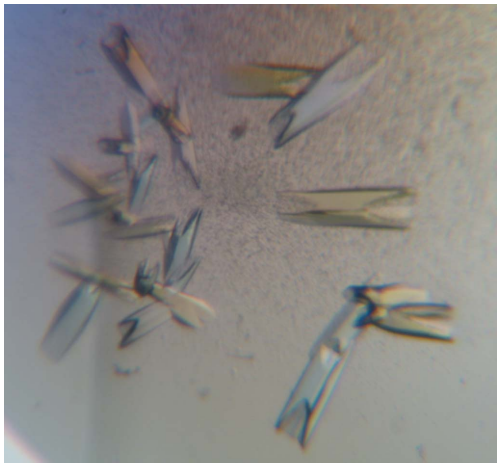

Figure 1
Native crystals of *H. pylori* MinE grown after 7 d in 100 m*M* MES–NaOH pH 6.5, 26%(*w*/*v*) PEG 3350. The crystal dimensions are approximately 0.2 × 0.1 × 0.1 mm.

2.2. Crystallization and data collection

H. pylori MinE was crystallized at room temperature (294 ± 1 K) using the hanging-drop vapour-diffusion method. Crystallization conditions for *H. pylori* MinE were initially screened using Crystal Screen, Crystal Screen 2 and Index (Hampton Research, USA). The optimized crystals were grown on a siliconized cover slip by equilibrating a mixture consisting of 1 µl protein solution (20 mg ml^{-1} protein in 20 m*M* Tris–HCl pH 6.0, 150 m*M* NaCl) and 1 µl reservoir solution [100 m*M* MES–NaOH pH 6.5, 26%(*w*/*v*) PEG 3350] against 500 µl reservoir solution. Crystals grew to maximum dimensions of 0.2 × 0.1 × 0.1 mm in a week (Fig. 1). They were cryoprotected in reservoir solution supplemented with 10%(*v*/*v*) glycerol and flash-cooled under N_2 gas at 95 K. Native data were collected to a resolution of 2.8 Å from each cooled crystal using an ADSC Quantum Q210 CCD detector on beamline 4A at the Pohang Accelerator Laboratory (PAL), Republic of Korea. Multiple anomalous dispersion (MAD) data sets were collected from SeMet-labelled crystals using an ADSC Quantum 315 CCD detector on beamline BL5 at the Photon Factory (PF), Japan. Four wavelengths (0.9796, 0.9791, 0.9833 and 0.9644 Å) were used for the MAD experiment. Data sets were processed and scaled using *HKL*-2000 (Otwinowski & Minor, 1997). The data-collection statistics are summarized in Table 1.

3. Results and discussion

H. pylori MinE crystals belonged to space group $P6_4$, with unit-cell parameters $a = b = 70.8$, $c = 65.5$ Å. Assuming the presence of two

molecules in the asymmetric unit, the calculated Matthews coefficient was 2.58 Å^3 Da^{-1}, which corresponds to a solvent content of 52.3% (Matthews, 1968). Initial molecular-replacement (MR) calculations were carried out with *MOLREP* (Vagin & Teplyakov, 1997) using the truncated *E. coli* MinE structure (residues 32–88; PDB code 1ev0; King *et al.*, 2000) as a search model. Attempts to determine the crystal structure of *H. pylori* MinE using MR were unsuccessful, probably because of the low sequence identity (28%) between the search model and *H. pylori* MinE.

For MAD phasing, a four-wavelength data set was collected at 3.0 Å resolution. The positions of the four Se atoms within the asymmetric unit were found using the program *SOLVE* (Terwilliger, 2003), yielding phases with a figure of merit (FOM) of 0.60 in the 20.0–3.0 Å resolution range. Density modification using the program *RESOLVE* (Terwilliger, 2003) improved the map quality and the FOM increased to 0.71. The experimental electron-density map was calculated at a resolution of 3.0 Å and was interpretable. Model building and further refinement are ongoing.

This work was supported by grants from the Gwangju Institute of Science and Technology Systems Biology Infrastructure Establishment and the Research Center for Biomolecular Nanotechnology at GIST.

References

Gitai, Z. (2007). *Curr. Opin. Cell Biol.* **19**, 5–12.
Huang, J., Cao, C. & Lutkenhaus, J. (1996). *J. Bacteriol.* **178**, 5080–5085.
King, G. F., Shih, Y. L., Maciejewski, M. W., Bains, N. P., Pan, B., Rowland, S. L., Mullen, G. P. & Rothfield, L. I. (2000). *Nature Struct. Mol. Biol.* **7**, 1013–1017.
Matthews, B. W. (1968). *J. Mol. Biol.* **33**, 491–497.
Moller-Jensen, J. & Lowe, J. (2005). *Curr. Opin. Cell Biol.* **17**, 75–81.
Otwinowski, Z. & Minor, W. (1997). *Methods Enzymol.* **276**, 307–326.
Pichoff, S., Vollrath, B., Touriol, C. & Bouche, J. P. (1995). *Mol. Microbiol.* **18**, 321–329.
Raskin, D. M. & de Boer, P. A. (1997). *Cell*, **91**, 685–694.
Raskin, D. M. & de Boer, P. A. (1999). *Proc. Natl Acad. Sci. USA*, **96**, 4971–4976.
RayChaudhuri, D., Gordon, G. S. & Wright, A. (2000). *Nature Struct. Mol. Biol.* **7**, 997–999.
Rothfield, L., Taghbalout, A. & Shih, Y. L. (2005). *Nature Rev. Microbiol.* **3**, 959–968.
Terwilliger, T. C. (2003). *Methods Enzymol.* **374**, 22–37.
Vagin, A. & Teplyakov, A. (1997). *J. Appl. Cryst.* **30**, 1022–1025.
Zhao, C. R., de Boer, P. A. & Rothfield, L. I. (1995). *Proc. Natl Acad. Sci. USA*, **92**, 4313–4317.